Emission Spectroscopy of AlH: the $X^1\Sigma^+$, $A^1\Pi$ and $C^1\Sigma^+$ States Characteristics

W. Szajna, M. Zachwieja, R. Hakalla and R. Kępa

Atomic and Molecular Physics Laboratory, Institute of Physics, University of Rzeszów

T. Rejtana 16A, 35-959 Rzeszów, Poland

The visible spectrum of AlH has been investigated at high resolution between 20000 and 21500 cm^{-1} using a conventional spectroscopic technique. The AlH molecules were formed and excited in an aluminium hollow-cathode lamp with two anodes, filled with a mixture of Ne carried gas and a trace of NH$_3$. The emission from the discharge was observed with a plane grating spectrograph and recorded by a photomultiplier tube. The 0–0 and 1–1 bands of the $C^1\Sigma^+$–$A^1\Pi$ system and 0–2 band of the $A^1\Pi$–$X^1\Sigma^+$ were identified at 21126, 21368 and 20276 cm^{-1}, respectively. In total 121 transition wave numbers belonging to three bands were precisely measured (with accuracy of ±0.003 cm^{-1}) and rotationally analysed. The new data were elaborated with the help of recent $X^1\Sigma^+$ state parameters reported by White et al. and of the $C^1\Sigma^+$, $A^1\Pi$ states constants reported by Szajna and Zachwieja. As a result of this merged analysis the set of the molecular parameters and rotational terms values for the three lower lying states of the AlH molecule have been significantly improved.

PACS: 33.20.Kf, 33.20.Vq

1. Introduction

There is a considerable experimental and theoretical interest in the spectra of metal-containing diatomic hydride molecules, because of their importance in several areas of science, including chemistry and astrophysics. For instance, aluminium hydride has properties that make it important in nuclear engineering, in the purification of metals, and in the preparation of electronically pure metal films, used as chemical reducing agents, and high-energy propellants. AlH has continued to be of interest to astronomers since its presence was detected in the emission spectra of sunspots [1] and atmospheres of M-, S-, Sp-, and C-type stars [2–4].

Since the first laboratory study of the spectrum of AlH in 1901 by Basquin [5] many electronic transitions have been identified in the visible and ultraviolet region (for review see [6] and references therein).

The $C^1\Sigma^+$–$A^1\Pi$ transition, near 4500 Å, was identified for the first time by Bengtsson and Hulthén in 1928 [7]. However, only strongest Q branch of the 0–0 band has been observed and no rotational analysis has been made. The $C^1\Sigma^+$ state is also known from the $C^1\Sigma^+$–$X^1\Sigma^+$ transition analyzed by Grabe and Hulthén [8], Khan [9] and by Zhu et al. [10]. More recently Szajna and Zachwieja [11] have made new registration and analysis of the 0–0, 1–1 and 1–2 bands of C–X transition and have provided precise values of the molecular constants for the excited state. The $A^1\Pi$–$X^1\Sigma^+$ transition has been the most extensively investigated system for many years. The most comprehensive investigation of this electronic transition was pro-

vided by Zeeman and Ritter [12]. They reported on the analysis of nine bands with $v = 0, 1$ in the $A^1\Pi$ state and $v = 0, 1, 2, 3, 4$ in the $X^1\Sigma^+$ state. From the graphical procedure they estimated values of principal molecular constants for both electronic states. The 0–0 and 1–1 bands were observed by Ram and Bernath [13] with a Fourier-transform spectrometer. They did not observe any off-diagonal bands due to the weak intensity of the off-diagonal transitions. More recently Zhu et al. [10] measured the absorption spectra of the $A^1\Pi$–$X^1\Sigma^+$ (0–0) transition in AlH by laser-induced fluorescence. In our previous study [6] we recorded six bands (0–0, 0–1, 1–0 to 1–3) of this system and conducted full rotational analysis. The vibration-rotation bands (from 1–0 to 5–4) of AlH have been observed using FTIR spectrometer by White et al. [14]. They give sets of the Dunham constants as well as mass-reduced Dunham parameters for the ground $X^1\Sigma^+$ state of AlH.

The electronic structure of the ground state and the first, low lying excited states of AlH has been the subject of numerous theoretical studies. The most accurate description of the $X^1\Sigma^+$, $A^1\Pi$ and $C^1\Sigma^+$ states from the complete active space self-consistent field (CASSCF) calculations have been reported by Matos et al. [15].

In the course of our work on aluminium hydride we have recorded a visible spectrum in the 20000 and 21500 cm^{-1}. We have identified and analysed the 0–0 band and the previously unobserved 1–1 band of the $C^1\Sigma^+$–$A^1\Pi$ transition and also 0–2 band of the $A^1\Pi$–$X^1\Sigma^+$ transition. The major objective of this work is to determine precise values of the wave numbers of lines of the C–A system, rotational terms values and also to

provide a consistent set of improved molecular constants for the three lowest singlet states of AlH.

2. Experimental details

The spectra of the $C^1\Sigma^+$–$A^1\Pi$ and $A^1\Pi$–$X^1\Sigma^+$ transitions of AlH were excited in a water-cooled aluminium hollow-cathode lamp with two anodes [16]. The anodes were operated at 2×490 V, 2×80 mA dc and extra electric field was added between anodes in order to convert one of them into a hollow-cathode (300 V, 140 mA dc). A non-flowing mixture of 2.5 Torr of Ne carried gas and a trace amount of NH$_3$ (≈ 0.2 Torr) was found as optimal for production of a strong spectrum.

The emission from the discharge was observed with the 2 m Ebert plane grating PGS-2 spectrograph in the 5th order. The reciprocal linear dispersion was about 0.090 nm/mm. The spectrum of AlH was recorded by translating on a linear stage an exit slit and photomultiplier tube (Hamamatsu R943-02) along the focal curve of the spectrograph. The entrance and exit slit widths were 0.035 mm. The line intensities were measured by a single photon counting with a counter gate time of 200–500 ms depending on spectrum intensity. Positions of the exit slit were measured using He–Ne laser interferometer synchronized with the photon counting board. The total number of the measurement points was about 73 000, for one 21 cm long scan with the sample step of 3 μm. In order to reduce the fluctuations of the line positions, the apparatus is thermally insulated and mounted on the main wall with channel iron and a 6 cm thick granite plate, whereas the temperature in the laboratory room is stabilized with an air conditioner and 0.2 degree centigrade accuracy. Repeatability of the line position measurements was tested to be 0.2–0.5 μm according to the variations of the atmospheric pressure.

Simultaneously recorded Th lines [17], obtained from several overlapped orders of the spectrum from a water--cooled hollow-cathode tube were used for absolute wavenumber calibration. Peak positions of the spectral lines were calculated by using the least-squares procedure and assuming Gaussian line shape to each spectral contour. For the wave-number calculations seventh-order interpolation polynomials were used. The typical standard deviation of the least-squares fit for the 35–45 calibration lines was about 0.0015–0.0020 cm^{-1}. The AlH lines have spectral widths of about 0.15–0.20 cm^{-1} and appear with a maximum signal-to-noise ratio of about 50 : 1 for the strongest bands. Consequently, the positions for strong and isolated lines were determined with an accuracy better than ± 0.003 cm^{-1}. However, some weaker and blended lines were measured with lesser precision of ± 0.006 cm^{-1}. In total, 121 lines belonging to 0–0, 1–1 bands of the $C^1\Sigma^+$–$A^1\Pi$ transition and 0–2 band of the $A^1\Pi$–$X^1\Sigma^+$ transition of AlH have been measured and their wave numbers are provided in Table I.

TABLE I

The wave numbers of the 0–0, 1–1 bands of the $C^1\Sigma^+$–$A^1\Pi$ system and 0–2 band $A^1\Pi$–$X^1\Sigma^+$ system of AlH[a].

J	$P_{11ee}(J)$	o–c	$Q_{11ef}(J)$	o–c	$R_{11ee}(J)$	o–c
0–0 band of $C^1\Sigma^+$–$A^1\Pi$						
1.0	21114.7579	42	21127.5445	−13	21153.0671	−3
2.0	21103.4571	48	21129.0433	31	21167.2717	56
3.0	21092.9167	35	21131.2949	70	21182.1579	−57
4.0	21083.1603	34	21134.2876	−87	21197.7619	74
5.0	21074.1954	−111	21138.0781	27	21214.0353	−11
6.0	21066.0850	−31	21142.6420	41	21230.9934	*
7.0	21058.8326	14	21148.0041	44	21248.6804	38
8.0	21052.4692	6	21154.1837	35	21267.0410	−35
9.0	21047.0414	35	21161.1997	−28	21286.1166	−65
10.0	21042.5750	−60	21169.0905	−38	21305.9274	7
11.0	21039.1402	−58	21177.8956	70	21326.5161	*
12.0	21036.8065	*	21187.6535	*	21347.7975	67
13.0	21035.5813	*	21198.3553	52	21369.9080	−1
14.0	21035.5813	*	21210.1204	−4	21392.8685	23
15.0	21036.8418	*	21223.0093	48	21416.7088	−67
16.0	21039.5611	5	21237.0784	−42	21441.5347	*
17.0	21043.7658	−127			21467.3462	−63
1–1 band of $C^1\Sigma^+$–$A^1\Pi$						
1.0	21357.8207	*	21369.4733	*		
2.0	21348.3139	−18	21371.6480	60	21406.4507	−96
3.0	21339.9723	−51	21374.9200	13	21421.1799	−88
4.0	21332.8066	33	21379.2977	69	21436.2656	#
5.0	21326.8380	77	21384.1139	#	21458.7614	#
6.0	21321.4743	#	21396.5773	#	21474.0618	#
7.0	21323.9078	#	21402.0204	#	21492.7847	#
0–2 band of $A^1\Pi$–$X^1\Sigma^+$						
0.0					20288.7392	0
1.0			20276.8489	−3	20300.9455	28
2.0	20253.1177	*	20277.1530	−15	20313.2793	−22
3.0	20241.6189	13	20277.5955	−3	20325.7257	−11
4.0	20230.2838	−17	20278.1541	13	20338.2433	7
5.0	20219.1183	−7	20278.7970	−12	20350.7852	−2
6.0	20208.0975	−13	20279.4958	−15	20363.3047	7
7.0	20197.1984	4	20280.2075	−2	20375.7379	−8
8.0	20186.3844	23	20280.8796	11	20388.0207	−1
9.0	20175.6105	28	20281.4499	2	20400.0725	13
10.0	20164.8176	−46	20281.8367	*	20411.8047	54
11.0	20153.9631	3	20281.9936	*	20423.1002	−13
12.0	20142.9559	11	20281.8030	*	20433.8590	2
13.0	20131.7112	10	20281.1496	−13	20443.9350	7
14.0	20120.1253	0	20279.9090	−37	20453.1696	−8
15.0	20108.0869	82	20277.9347	−58	20461.3824	−20
16.0	20095.4298	23	20275.0454	*	20468.3529	*
17.0	20082.0041	3	20271.0761	69		
18.0	20067.6015	−87				

[a] In cm^{-1}, observed minus calculated values are shown in the columns labeled o–c.

* Indicates low accuracy lines not included in the fit.

# Indicates perturbed lines not included in the fit. Perturbations in the $C^1\Sigma^+$, $v = 0, 1$ state which have been theoretically predicted in work [15] were experimentally confirmed and precisely described in our previous work [11].

3. Description of the spectra

The bands of the $^1\Pi$–$^1\Sigma^+$ and $^1\Sigma^+$–$^1\Pi$ transitions have a very simple and similar structure: single P-, single Q-, and single R-branch. The main difference between these bands is that for the former the rotational lines $P(0)$, $P(1)$ and $Q(0)$ are missing, whereas, for the latter, $P(0)$, $R(0)$ and $Q(0)$ are missing (see Figs. 1 and 2).
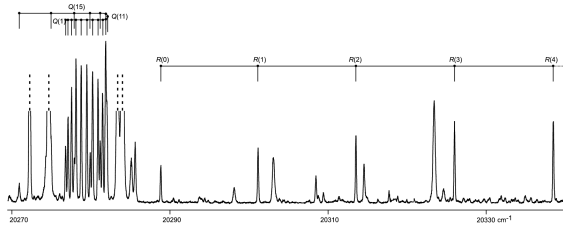

Fig. 1. An expanded portion of the spectrum of the 0–2 band of the $A^1\Pi$–$X^1\Sigma^+$ system of AlH near the Q head. The strongest atomic lines are marked with a broken line.
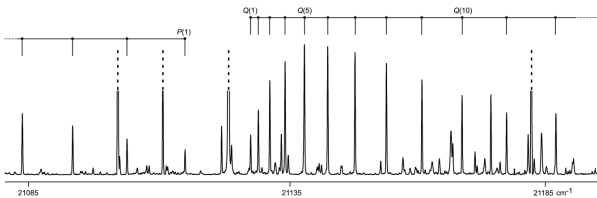

Fig. 2. An expanded portion of the spectrum of the 0–0 band of the $C^1\Sigma^+$–$A^1\Pi$ system of AlH near the band origin. The strongest atomic lines are marked with a broken line.

3.1. The $A^1\Pi$–$X^1\Sigma^+$ transition of AlH

The band observed with the origin at 20276.69315 (45) cm^{-1}, has been recognized as the 0–2 band of the $A^1\Pi$–$X^1\Sigma^+$ transition. This band has been firstly assigned by Holst [18] as the 0–0 band of the new $B^1\Sigma^-$–$A^1\Pi$ transition. The hypothesis of the $B^1\Sigma^-$ state existence, suggested by Holst was refuted by Zeeman and Ritter [12]. The part of the band spectrum with the characteristic head in the Q branch is presented in Fig. 1. The rotational lines of the 0–2 band could not be followed up to $P(18)$, $Q(17)$, and $R(16)$ due to predissociation in the $A^1\Pi(v=0, J=17)$ state.

3.2. The $C^1\Sigma^+$–$A^1\Pi$ transition of AlH

The bands with the origins at 21126.7997(16) and 21368.3654 (35) cm^{-1}, have been assigned as the previously observed 0–0 and new one 1–1 bands of the $C^1\Sigma^+$–$A^1\Pi$ transition, respectively. Because of the predissociation in the A state mentioned above, both bands are sharply cut off in the intensity of rotational lines at $J'' = 17$ and $J'' = 7$, respectively (see line positions

in Table I). The 1–1 band has about 25% of the intensity of the strongest 0–0 band. The part of the P and Q branches of the 0–0 band is presented in Fig. 2, where clearly resolved lines are rotationally interpreted.

4. Analysis and results

The obtained molecular constants for the $X^1\Sigma^+$, $A^1\Pi$ and $C^1\Sigma^+$ states will be presented and discussed in this section.

4.1. Molecular constants determination

Initially, band-by-band fits were made via a linear least-squares procedure and using the observed line positions showed in Table I. The following customary energy level expressions for $^1\Sigma^+$ (1) and $^1\Pi$ (2) states was used:

$$F_v(J) = T_v + B_v J(J+1) - D_v \left[J(J+1)\right]^2$$
$$+ H_v \left[J(J+1)\right]^3 + L_v \left[J(J+1)\right]^4, \qquad (1)$$

$$F_v(J) = T_v + B_v J(J+1) - D_v \left[J(J+1)\right]^2$$
$$+ H_v \left[J(J+1)\right]^3 + L_v \left[J(J+1)\right]^4$$
$$\pm \frac{1}{2}\left\{q_v J(J+1) + q_{D_v} \left[J(J+1)\right]^2\right\}, \qquad (2)$$

with the plus sign for e-levels and the minus sign for f-levels in the Λ-doubling terms of the $^1\Pi$. During an individual band analysis, it was noted that wave numbers of the lines deviated from the model and were not included in the fit (see line positions in Table I).

The calculations of the final molecular parameters, bands origins and vibration terms values for the observed levels were performed by the least-squares merge fit described by Albritton et al. [19] and by Coxon [20]. Such merging is equivalent to a global fit of all data parameters sets for all states but it is more careful and makes it possible to find prospective strong correlations between molecular parameters or systematic errors of wave numbers measurements. As an input data of these calculations, we used present data and recently published by us results dealing with $A^1\Pi$–$X^1\Sigma^+$ [6] and $C^1\Sigma^+$–$X^1\Sigma^+$ [11] transitions and (refitted by us) data of the high-resolution measurements of the vibration-rotation bands of the $X^1\Sigma^+$ state given by White et al. [14].

Merging was performed in two steps. In the first one (named A), fourteen bands origins and 124 molecular constants obtained from individual bands analysis were reduced up to 62 parameters: 14 band origins, 9 vibrational terms values and 39 rotational constants characterizing the nine vibrational levels of the $X^1\Sigma^+$, $v = 0$–5, $A^1\Pi$, $v = 0, 1$ and $C^1\Sigma^+$, $v = 0$ states, respectively.

Next, we used molecular constants (obtained in the previous step) for the $X^1\Sigma^+$, $v = 1, 2$ and $A^1\Pi$, $v = 1$ state as help in the individual fits of the 1–1, 1–2 bands of the C–X and 1–1 band of the C–A systems, with a common upper vibrational level. All molecular constants for the lower vibrational level ($v = 1, 2$ in X state and $v = 1$ in A state, respectively) were fixed to the values obtained

in merge A. We have chosen this procedure because the latter three bands are very short and also strongly perturbed [11]. Experimental data were not sufficient to allow us to do the simultaneous determination of the molecular parameters for both states with satisfactory precision.

In that way we obtained molecular parameters for the $C^1\Sigma^+$, $v = 1$ level only. The constants found from the individual fits of the three mentioned bands have been taken as input data in merge B and the single-value of the molecular constants for the $C^1\Sigma^+$, $v = 1$ level have been extracted. Also, three values of the bands origins and vibrational term value of the $v = 1$ of the C state were derived. The obtained molecular constants for the $C^1\Sigma^+(v = 0,1)$, $A^1\Pi(v = 0,1)$ and $X^1\Sigma^+(v = 0\text{–}5)$ states are listed in Table II, while the bands origins values are summarized in Table III.

TABLE II

Molecular constants for the $C^1\Sigma^+$, $A^1\Pi$ and $X^1\Sigma^+$ states of AlH[a].

v	T_v	B_v	$D_v \times 10^4$	$H_v \times 10^6$	$L_v \times 10^{10}$	$q_v \times 10^3$	$q_{D_v} \times 10^6$
			$C^1\Sigma^+$ state				
1	45922.0436(20)	5.83037(51)	11.37(24)				
0	44597.7072(28)	6.388805(51)	5.2954(40)	−0.0212(11)	0.5617(78)		
			$A^1\Pi$ state				
1	24553.68193(71)	5.287606(66)	11.145(27)	−1.416(31)		6.894(35)	−5.81(71)
0	23470.90633(55)	6.020146(18)	6.3126(26))	−0.0658(13)	−1.619(22)	8.2996(52)	−3.332 (22)
			$X^1\Sigma^+$ state[b]				
5	7579.56467(52)	5.4182473(94)	3.34371(86)	0.01443(28)	−0.0135(28)		
4	6170.19408(16)	5.5880741(17)	3.401175(76)	0.014188(13)	−0.007934(70)		
3	4708.818208(96)	5.76108361(98)	3.462567(39)	0.0144661(63)	−0.007930(41)		
2	3194.214047(37)	5.93744077(69)	3.525349(28)	0.0146806(55)	−0.007855(44)		
1	1625.069576(22)	6.11728783(69)	3.589210(28)	0.0148845(56)	−0.007961(49)		
0	0.0	6.30071641(74)	3.653558(31)	0.0150672(58)	−0.008165(55)		

[a] In cm^{-1}, 1σ in parentheses.

[b] The $X^1\Sigma^+$ state parameters were obtained with help of the experimental data reported by White et al. [14].

TABLE III

The observed bands origins of the $A^1\Pi$–$X^1\Sigma^+$, $C^1\Sigma^+$–$X^1\Sigma^+$ and $C^1\Sigma^+$–$A^1\Pi$ transition of AlH[a].

		$X^1\Sigma^+$			
		$v = 0$	$v = 1$	$v = 2$	$v = 3$
$A^1\Pi$	$v = 0$	23470.90610(31)	21845.83842(50)	20276.69315(45)	
	$v = 1$	24553.68132(41)	22928.61289(42)	21359.46887(70)	19844.86617(70)
$C^1\Sigma^+$	$v = 0$	44597.7142(22)			
	$v = 1$		44296.9738(20)	42727.8361(67)	
		$A^1\Pi$			
$C^1\Sigma^+$	$v = 0$	21126.7997(16)			
	$v = 1$		21368.3654(35)		

[a] In cm^{-1}, 1σ in parentheses.

The excited states main rotational constants agree well with the previous experimental results [8, 10, 12, 13]. For example, our $B_0 = 6.388805(51)$ cm^{-1} constant of C state compares with values of 6.393 cm^{-1} [8] and 6.3870 cm^{-1} [10]. However, obtained constants of C, $v = 1$ (especially $D_1 = 11.37(24) \times 10^{-4}$ cm^{-1}) has to be treated with great care due to the wide perturbations observed in 1–v'' progression bands of C–X and C–A systems. Present $A^1\Pi(v = 1)$ level parameters (i.e. D_1, H_1) differ from those of work [13], and are closer to the results obtained by Zeeman and Ritter [12]. For example, our $D_1 = 11.145(27) \times 10^{-4}$ cm^{-1} constants in comparison with the values $11.195_0 \times 10^{-4}$ cm^{-1} [12] and $11.45(11) \times 10^{-4}$ cm^{-1} [13], respectively.

The present ground state constants, for the $v = 0, 1$ are in good agreement with the values of Ram and Bernath [13]. This is not surprising as the same experimental material (0–0, 1–1 bands of the A–X system and 1–0 vibration-rotation band) has been partially used in both studies.

4.2. Equilibrium parameters of the $X^1\Sigma^+$, $A^1\Pi$ and $C^1\Sigma^+$

On the basis of the obtained values of rotational constants, and assuming their traditionally recognised polynomial dependence of the vibrational quantum number, by means of calculations based on the weighted least-squares method the equilibrium molecular parameters for the $X^1\Sigma^+$, $A^1\Pi$ and $C^1\Sigma^+$ state were calculated. Because only $v = 0$ and 1 levels have been observed in the $A^1\Pi$ and $C^1\Sigma^+$ states, the equilibrium constants for this state were determined from a fit of the data in which the number of data equal the number of determined parameters (sometimes called the exact fit). In that case standard deviations of equilibrium parameters were calculated by means of the Gauss error propagation method.

The main equilibrium rotational constants (B_e, D_e) of the $A^1\Pi$ and $C^1\Sigma^+$ states can be compared with the available results of previous experimental work [12, 13] and [8], respectively. Our $B_e = 6.386416(43)$ cm^{-1} constant of A state agrees well with those of Zeeman and Ritter [12] of $B_e = 6.3868_8$ cm^{-1} and Ram and Bernath [13] of $B_e = 6.38632(14)$ cm^{-1}, respectively. The present $B_e = 6.66802(27)$ cm^{-1} constant of C state confirms the value of $B_e = 6.664$ cm^{-1} reported by Grabe and Hulthén [8]. The ground state equilibrium parameters are in acceptable compatibility (within the double standard deviation) with the most precise results given by White et al. [14] from AlH and AlD infrared spectrum. Some of our equilibrium constants (i.e. ε_e, δ_e, β_{He}) have been statistically undetermined (were smaller than their uncertainties), and these constants have been fixed to zero values.

The vibrational terms values of the $X^1\Sigma^+$, $A^1\Pi$ and $C^1\Sigma^+$ states (relative to the $X^1\Sigma^+$, $v = 0$ level) have been used to calculate the equilibrium vibrational constants for three states. The σ_e and ω_e constants of the excited states have been calculated with the fixed values of the $\omega_e x_e$ constants (for detail see footnote of Table IV). For the ground state parameters (ω_e, $\omega_e x_e$, $\omega_e y_e$, and $\omega_e z_e$) determination we used the constrained values of the $Y_{50} = -1.3 \times 10^{-4}$ cm^{-1} from the investigation of the infrared emission spectra of AlH [14]. The obtained equilibrium parameters of X, A and C state of AlH are displayed in Table IV.

5. Rotational terms determination

In order to systematize and complete information about three low lying singlet states of AlH i.e. $C^1\Sigma^+$, $A^1\Pi$ and $X^1\Sigma^+$, the rotational terms values have been calculated. In the absence of perturbations in the $X^1\Sigma^+$,

TABLE IV

Equilibrium molecular constants for the $X^1\Sigma^+$, $A^1\Pi$ and $C^1\Sigma^+$ states of AlH[a].

Constant	$X^1\Sigma^+$	$A^1\Pi$	$C^1\Sigma^+$
σ_e	–	23638.32912(90)	44675.3696(44)
ω_e	1682.37499(17)	1416.49560(90)	1575.3364(35)
$\omega_e x_e$	29.05111(15)	166.86[b]	125.5[c]
$\omega_e y_e$	0.247654(44)		
$\omega_e z_e \times 10^3$	$-1.4152(44)$		
$Y_{50} \times 10^4$	-1.3^d		
B_e	6.3937898(20)	6.386416(43)	6.66802(27)
α_e	0.1870560(30)	0.732540(69)	0.55844(52)
$\gamma_e \times 10^3$	1.8186(11)		
ε_e	0.00[e]		
$\eta_e \times 10^6$	$-1.922(26)$		
$D_e \times 10^4$	3.685885(70)	3.896(14)	2.26(12)
$\beta_e \times 10^4$	$-0.064627(50)$	4.832(28)	6.07(24)
δ_e	0.00[e]		
$\zeta_e \times 10^9$	6.71(27)		
$H_e \times 10^7$	0.15156(11)	6.09(16)	
$\alpha_{He} \times 10^6$	$-0.0001778(77)$	$-1.350(31)$	
β_{He}	0.00[e]		
$\gamma_{He} \times 10^{12}$	$-1.72(41)$		
$L_e \times 10^{13}$	8.272(82)		
$\alpha_{Le} \times 10^{14}$	$-2.69(75)$		
$\beta_{Le} \times 10^{15}$	4.6(16)		
$q_e \times 10^3$		9.002(20)	
$\alpha_{q_e} \times 10^3$		$-1.406(36)$	
$q_{De} \times 10^6$		$-2.09(36)$	
$\alpha_{q_{De}} \times 10^6$		$-2.48(71)$	
r_e	1.64735188(26)	1.6483026(55)	1.613122(33)^f

[a] In cm^{-1}, r_e in Å, 1σ in parentheses.
[b] Fixed to the value recalculated from the AlD parameter [21].
[c] Fixed to the value reported by Grabe and Hulthén [8].
[d] Fixed to the value reported by White et al. [14].
[e] Fixed to the zero value due to statistical indeterminacy.
[f] Inner minimum of the $C^1\Sigma^+$ state.

$v = 0$–5 state and in the $A^1\Pi$, $v = 0$ state of AlH [6, 14] the rotational terms values for these states were calculated on the basis of presently obtained molecular constants (Table II). The wide results for the $X^1\Sigma^+$ state are available from our webside [22], while for the $A^1\Pi$, $v = 0$ are featured in Table V. Because $A^1\Pi$, $v = 1$ and $C^1\Sigma^+$, $v = 0, 1$ states are suspected of irregularities [6, 11] the rotational terms values for these states were calculated by means of the method introduced by Curl and Dane [23] and Watson [24]*. In this procedure, terms values of the vibrational level of the C and A states have been calculated on the basis of molecular constants

———

* They described the unbiased least-squares procedure for fitting spectra with perturbed upper states which involves an initial determination of lower-state constants and upper state term values followed by a determination of upper-state constants from the term values.

of the $X^1\Sigma^+$ state and wave numbers of observed lines of the 1–0, 1, 2, 3 bands of A–X system and 0–0, 1–1, 2 bands of the C–X system (all the perturbed lines of the mentioned bands have been included in the fit). The observed wave numbers of the bands of the A–X and C–X system were compared in individual calculations with appropriate differences of the rotational terms of the upper and lower state. The rotational terms of the upper states were parameters determined, while the lower state terms ($X^1\Sigma^+$, $v = 0$–3) were calculated on the basis of constrained molecular constants in accordance with Eq. (1). Next, the average weighted terms values of the $A^1\Pi$, $v = 1$ and $C^1\Sigma^+$, $v = 0, 1$ levels were determined. The results are featured in Table V.

TABLE V

Rotational term values for the $A^1\Pi$, $v = 0, 1$ and $C^1\Sigma^+$, $v = 0, 1$ states of AlH[a].

J	$A^1\Pi$, $v = 0$		$A^1\Pi$, $v = 1$		$C^1\Sigma^+$, $v = 0$	$C^1\Sigma^+$, $v = 1$
	F_{1e}	F_{1f}	F_{1e}	F_{1f}	F_{1e}	F_{1e}
0	23470.9061	23470.9061			44597.7097(21)	45922.0803(46)
1	23482.9522	23482.9356	24564.2606(12)	24564.2458(5)	44610.4833(21)	45933.7053(46)
2	23507.0291	23506.9794	24585.3882(8)	24585.3469(10)	44636.0223(18)	45956.9906(39)
3	23543.1064	23543.0073	24617.0122(7)	24616.9303(10)	44674.3008(18)	45991.7447(33)
4	23591.1383	23590.9736	24659.0458(12)	24658.9083(6)	44725.2623(18)	46038.2008(37)
5	23651.0634	23650.8174	24711.3647(10)	24711.1912(5)	44788.8956(18)	46095.3127(37)
6	23722.8047	23722.4620	24773.8307(5)	24773.5520(10)	44865.1022(18)	46170.1271(37)
7	23806.2687	23805.8143	27846.2296(16)	27845.8610(8)	44953.8175(21)	46247.8823(37)
8	23901.3454	23900.7651			45054.9498(18)	46339.0505(46)
9	24007.9074	24007.1874			45468.3867(18)	46440.5943(59)
10	24125.8089	24124.9363			45294.0262(18)	
11	24254.8845	24253.8470			45431.7409(21)	
12	24394.9476	24393.7340			45581.3934(21)	
13	24545.7885	24544.3883			45742.7457(21)	
14	24707.1718	24705.5758			45915.6978(21)	
15	24878.8335	24877.0335			46100.0424(18)	
16	25060.4775	25058.4665			46295.5433(18)	
17	25251.7705	25249.5428			46502.0165(28)	
18					46719.1188(30)	
19					46946.6784(52)	
20					47184.1540(52)	
21					47431.6612(52)	
22					47688.7212(74)	
23					47952.1086(52)	
24					48227.5657(74)	
25					48509.9912(74)	
26					48800.0940(52)	
27					49097.4432(52)	
28					49400.4931(52)	

[a] In cm^{-1}, 1σ in parentheses.

6. Conclusions

High resolution spectra of the $C^1\Sigma^+$–$A^1\Pi(0$–0, 1–1$)$ and $A^1\Pi$–$X^1\Sigma^+(0$–2$)$ transitions of AlH have been observed by using a conventional spectroscopic technique. The 0–0 and 0–2 bands have been observed previously, while the 1–1 band of the C–A system has been observed and analysed for the first time. As the result of multistage and merged analysis of the currently obtained bands and of the bands obtained earlier [14, 6, 11] the information about $C^1\Sigma^+$, $A^1\Pi$ and $X^1\Sigma^+$ states of the AlH molecule has been enlarged and improved.

References

[1] P. Sotirovski, *Astron. Astrophys. Suppl.* **6**, 85 (1972).

[2] P.W. Merrill, *Astrophys. J.* **118**, 453 (1953).

[3] G. Herbig, *Pub. Astron. Soc. Pac.* **68**, 204 (1956).

[4] H.R. Johnson, A.J. Sauval, *Astron. Astrophys. Suppl. Ser.* **49**, 77 (1982).

[5] O.H. Basquin, *Astrophys. J.* **14**, 1 (1901).

[6] W. Szajna, M. Zachwieja, *Eur. Phys. J. D* **55**, 549 (2009).

[7] E. Bengtsson, E. Hulthén, *Z. Phys.* **52**, 275 (1928).

[8] B. Grabe, E. Hulthén, *Z. Phys.* **114**, 470 (1939).

[9] M.A. Khan, *Proc. Phys. Soc.* **71**, 65 (1958).

[10] Y. Zhu, R. Shehadeh, E. Grant, *J. Chem. Phys.* **97**, 883 (1992).

[11] W. Szajna, M. Zachwieja, *J. Mol. Spectrosc.* **260**, 130 (2010).

[12] P.B. Zeeman, G.J. Ritter, *Can. J. Phys.* **32**, 555 (1954).

[13] R.S. Ram, P.F. Bernath, *Appl. Opt.* **35**, 2879 (1996).

[14] J.B. White. M. Dulick, P.F. Bernath, *J. Chem. Phys.* **99**, 8371 (1993).

[15] J.M.O. Matos, P.-A. Malmqvist, B.O. Roos, *J. Chem. Phys.* **86**, 5032 (1987).

[16] R. Bacis, *J. Phys. E, Sci. Instrum.* **9**, 1081 (1976).

[17] B.A. Palmer, R. Engleman Jr., *Atlas of the Thorium Spectrum Los Alamos National Laboratory*, Los Alamos (NM) 1983, unpublished.

[18] V.W. Holst, *Z. Phys.* **90**, 735 (1934).

[19] D.L. Albritton, A.L. Schmeltekopf, R.N. Zare, *J. Mol. Spectrosc.* **67**, 132 (1977).

[20] J.A. Coxon, *J. Mol. Spectrosc.* **72**, 252 (1978).

[21] G. Herzberg, *Molecular Spectra and Molecular Structure I. Spectra of Diatomic Molecules*, Van Nostrand, 1950.

[22] `http://www.if.univ.rzeszow.pl/∼zfaim/dane.htm#AlH` .

[23] R.F. Curl, C.B. Dane, *J. Mol. Spectrosc.* **128**, 406 (1988).

[24] J.K.G. Watson, *J. Mol. Spectrosc.* **138**, 302 (1989).